Development of Infrared Detectors Using Single Carbon-Nanotube-Based Field-Effect Transistors

Hongzhi Chen, *Student Member, IEEE*, Ning Xi, *Fellow, IEEE*, King W. C. Lai, *Member, IEEE*, Carmen K. M. Fung, *Member, IEEE*, and Ruiguo Yang, *Student Member, IEEE*

***Abstract*—Carbon nanotube is a promising material to fabricate high-performance nanoscale-optoelectronic devices owing to its unique 1-D structure. In particular, different types of carbon-nanotube-infrared detectors have been developed. However, most previous reported carbon-nanotube-IR detectors showed poor device characteristics due to limited understanding of their working principles. In this paper, three types of IR detectors were fabricated using carbon-nanotube field effect transistors (CNTFETs) to investigate their performance: 1) symmetric Au-CNT-Au CNTFET IR detector; 2) symmetric Ag-CNT-Ag CNTFET IR detector; and 3) asymmetric Ag-CNT-Au CNTFET IR detector. The theoretical analyses and experimental results have shown that the IR detector using an individual single-wall carbon nanotube (SWCNT), with asymmetric Ag-CNT-Au CNTFET structure, can suppress dark current and increase photocurrent by electrostatic doping. As a result, an open-circuit voltage of 0.45 V under IR illumination was generated, which is the highest value reported to date for an individual SWCNT-based photodetector. The results reported in this paper have demonstrated that the CNTFET can be used to develop high-performance IR sensors.**

***Index Terms*—Carbon nanotube (CNT), field-effect transistor, IR detector, optoelectronics.**

I. Introduction

CARBON nanotubes (CNT) have been extensively explored since the first report in the early 1990s [1]. They have been widely used as the building blocks for biosensors [2], [3], gas sensors [4], [5], pressure sensors [6], [7], transistors [8], [9], light emitters [10], and photodetectors [11], [12] due to their excellent physical, electrical, and mechanical properties. In particular, the 1-D hollow-cylindrical structure of the single-wall carbon nanotube (SWCNT) possesses exceptional optoelectronic properties. The noise of 1-D photodetectors using SWCNT can be extremely low due to the phonon-scattering suppression [13] and size shrinkage [14]. This 1-D structure with high surface-to-volume ratio can inherently increase the SNR with prolonged photocarrier life time and shortened carrier-transit time [15], which may lead to a higher operation temperature that is significant for long wavelength photodetectors. The peak responsivity of the detectors can be tuned to the desired wavelength by controlling the diameter of CNTs, since the bandgap energy is inversely proportional to the diameter in quantum-confined structures [16], and the diameter of CNTs can be easily tailored by electrical breakdown [17], [18]. The dominant Fermi level pinning effect in planar contact is trivial in the 1-D structure [19]; thus, the performance of CNT-IR detectors can be improved by selecting proper metals.

IR detection using CNT thin film were first realized and reported in [20] and [21]. However, mixture of metallic and semiconductor CNTs as well as adsorbed oxygen severely degraded their photoresponse, thus, IR detectors using individual CNT were desired. Photoconductivity of a single SWCNT based p-n junction photodiode was observed by fabricating two split gates underneath both ends of the nanotube [22]. It was demonstrated that 1-D Schottky diodes between an individual SWCNT and metals were responsible for the photocurrent generation under continuous IR illumination [23], but the performance of the CNT Schottky photodiode was constrained by the work-function variation from technique difficulties in controlling CNT growth [24]. Therefore, doping level of nanotubes needs to be controlled in order to optimize CNT detector's performance. Carbon-nanotube field-effect transistors (CNTFETs) were developed to examine the photoconductivity by modulating the doping level electrostatically through a gate [25]–[27]. However, these CNTFETs focused on exploring the physics of the nanotubes, no study was primarily concentrated on optimizing CNT photosensor performance. In this paper, how to improve SWCNT detector's sensitivity using Schottky barriers modulated CNTFETs will be introduced. In particular, these devices are capable of enhancing both photocurrent and open-circuit voltage by controlling the 1-D Schottky barriers within nanotubes.

A review of the fundamentals of nanotube photodiode will be given first. The basic structure of a CNT photodiode is shown in Fig. 1(a), with a nanotube bridging two Au electrodes on a substrate. When a CNT comes into contact with metals, 1-D Schottky barriers may be formed within the nanotube, which are responsible for separating photoexcited electron-hole pairs in order to generate photocurrent. Fig. 1(b) and (c) shows the IR detection of a SWCNT photodiode by radiating IR photons on its left and right contacts. One distinct characteristic is the photocurrent (current difference between laser ON and OFF) changes direction but keep similar magnitude (1.5×10^{-11} A) when the laser illuminated at two different contacts. This is

Manuscript received December 31, 2009; revised April 21, 2010; accepted May 21, 2010. Date of publication June 17, 2010; date of current version September 9, 2010. This research work is supported in part by the National Science Foundation under Grant IIS 0713346, ONR Grant N00014-07-1-0935, and Grant N00014-04-1-0799. The review of this paper was arranged by Associate Editor C. Zhou.

The authors are with the Department of Electrical and Computer Engineering, Michigan State University, East Lansing, MI 48824 USA (e-mail: chenhon5@msu.edu; xin@egr.msu.edu; kinglai@egr.msu.edu; carmen@egr.msu.edu; yangruig@msu.edu).

Color versions of one or more of the figures in this paper are available onlne at http://ieeexplore.ieee.org.

Digital Object Identifier 10.1109/TNANO.2010.2053216

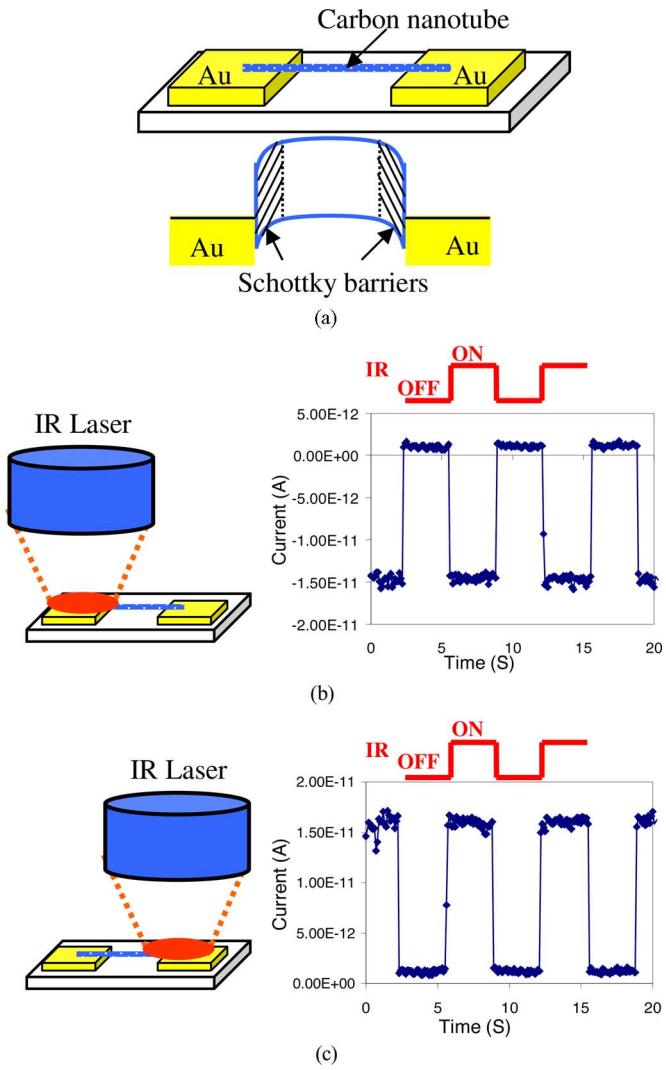

Fig. 1. (a) SWCNT photodiode and its corresponding band diagram. (b) and (c) Photoresponse with IR laser illuminating at left and right Schottky barriers at zero bias.

caused by the symmetric contacts between Au electrodes and CNT at both ends, forming two Schottky diodes inversely connecting to each other, as indicated in the band diagram in Fig. 1(a), more detailed discussion can be found in [23]. However, this photodiode has two primary problems that severely constrain its sensitivity. First, the Fermi level randomness originated from the growth techniques may render the detectors unworkable, since the Schottky barrier is determined by the energy level alignment between a metal and a nanotube. Second, the symmetric structure of two reversely connecting Schottky diodes will significantly suppress photocurrent generation.

In order to overcome the first problem, Fermi level of CNTs needs to be controlled. CNTFET has been demonstrated as an effective device to modulate the Schottky barriers by modifying the Fermi level of the CNTs using a gate [28], [29]. Instead of two Schottky barriers opposite to each other, one of the Schottky barriers needs to be alleviated or eliminated in order to enhance the photocurrent, which can be achieved by using two different metals at both ends of a nanotube. In this paper, how to optimize the detector's performance using CNTFET and asymmetric structure will be presented. First, the introduction of how to improve the performance of symmetric Au-CNT-Au CNTFET photodetectors using electrostatic doping by the gates of transistors will be given. The work function of metal is also found to play a vital role in determining its performance by examining the performance of a symmetric Ag-CNT-Ag photodetector. Asymmetric Ag-CNT-Au CNTFET using different metals as source and drain demonstrated extremely high open-circuit voltage (0.45 V), the highest value reported for a single SWCNT-based photodetector to date.

II. CNTFET Infrared Detectors

The theory of planar contact between metals and traditional semiconductors cannot be applied to the 1-D structures due to the quantum effects [30], thus, the behavior of nanotube photodetector is different from traditional photovoltaic devices. In this section, how to improve the performance of 1-D photodetectors using CNTFETs will be introduced.

A. CNTFET Design for Infrared Detectors

1-D Schottky barrier between a metal and a CNT is responsible for generating photocurrent in CNT photodetectors. The properties of the barrier are determined by the energy alignment at the contact. However, the work function of each individual nanotube may be different due to the diameter or chirality variation, accident doping from environment, and synthesis technique difference [31]–[33]. In other words, the photodetectors using as-synthesis CNTs may have poor performance due to the work-function randomness. Therefore, the work function of nanotube needs to be controlled so as to optimize the Schottky barrier for absorbing photons. The CNTFET has been demonstrated as a device that was operated by electrostatically modulating the Schottky barriers. The CNTFET with back-gate geometry, howbeit simple, can effectively control the Fermi energy of the nanotube and is easier to fabricate. In addition, this structure can be used to tailor the work function of nanotubes through chemical doping [34].

Fig. 2(a) shows a nanotube-IR detector with back-gate structure. In this configuration, a semiconductor CNT connects two-metal electrodes on a heavily doped Si/SiO_2 substrate. Two-metal contacts serve as the source and drain electrodes, while the conducting substrate is used as a gate terminal.

The fabrication process of this device began with fabricating source and drain electrodes using photolithography, thermal evaporation, and lift-off on top of a heavily doped silicon substrate covered with 200 nm SiO_2. The gap between two electrodes was around 1–2 μm. After that, a droplet of SWCNTs suspension (ethanol) was dropped to the gap between electrodes that connects to the dielectrophoresis (DEP)-deposition system [35]. An individual SWCNT was deposited between the electrodes assisted by the atomic-force microscope (AFM)-manipulation system [36]–[38]. A more detailed fabrication process was discussed in [39] and [40]. Fig. 2(b) shows an AFM image of a detector with an SWCNT connecting to the two-metal electrodes.

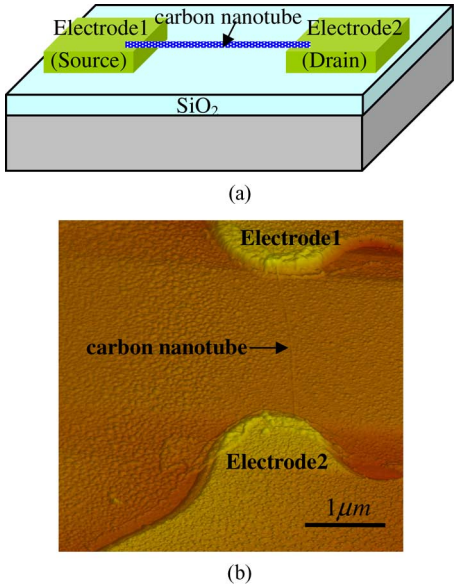

Fig. 2. (a) Symmetric back-gate CNTFET IR detector. (b) Corresponding AFM image.

If the material of both electrodes contacting the nanotube is the same, it is denoted as a symmetric CNTFET. This structure can not only be used to explore the role of work functions of both metal and nanotube, but also improve detector performance. However, two Schottky barriers will be symmetrically modulated by a gate in this structure, which will degrade the detector response. The asymmetric CNTFET can improve its photoresponse by using two metals with high/low work function as the source and drain electrodes. More discussion of these CNTFETs will be given in the following sections.

B. Symmetric Au-CNT-Au and Ag-CNT-Ag CNTFET Infrared Detectors

A symmetric Au-CNT-Au CNTFET IR detector using a 1.4-nm SWCNT was fabricated, its electrical characteristics with five different gate voltages are shown in Fig. 3(a). A quasi-metallic *I–V* characteristic (weak parabolic) was observed at zero gate voltage, which is resulted from two small Schottky barriers reversely connecting between the source and drain. The work function of Au is close to the Fermi energy of SWCNTs ($\sim$5.0 eV) [41], thus, small built-in potential was formed without gate voltage, leading to the weak Schottky barriers [42].

This transistor showed p-FET characteristic: negative gate voltage increased the conductance, while positive gate voltage decreased the conductance, as shown in Fig. 3. An exceptional characteristic is that the negative gate voltage resulted in linear *I–V* relationship, while positive gate voltage led to a current rectifying effect as a diode. Thermally assist tunneling through the barriers dominates the current injection in 1-D structure [43], therefore, the linear *I–V* at negative gate voltage indicated an extreme thin or zero barrier, whereas the barriers were enlarged by the positive gate voltage [44].

The photoresponse was measured by focusing an IR laser on one of the electrodes. The IR laser used has 830 nm wavelength

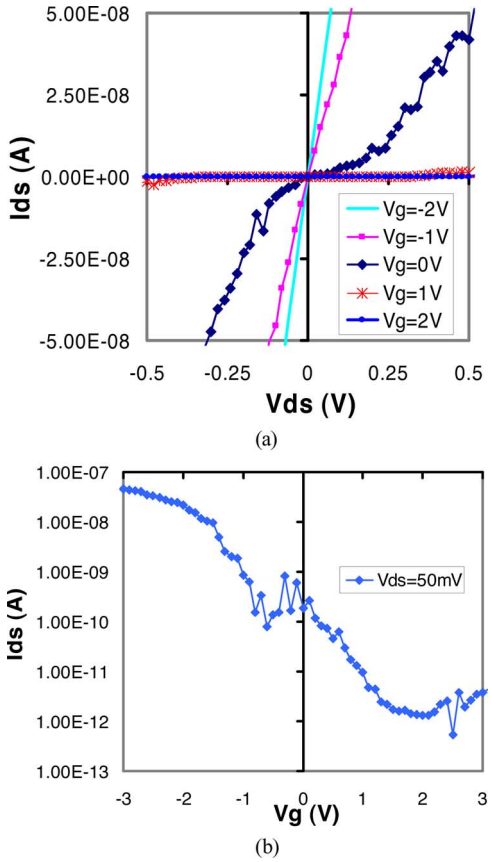

Fig. 3. (a) *I–V* characteristics of the CNTFET. (b) Transfer characteristics at $V_{ds} = 50$ mV.

and a maximum power of 50 mW. A more detailed introduction of the testing system can be found in [39]. Fig. 4(a) shows the transfer characteristics of the symmetric Au-CNTFET with IR laser OFF and ON at zero bias. It was observed that the dark current $(\mathrm{IR} = 0)$ increased with negative gate voltage, while decreased with positive gate voltage, corresponding to the change of conductance in Fig. 3(b). However, the transistor possessed drastically different transfer characteristics when IR laser was turned on. This indicated that IR-laser illumination generated excess carriers that contributed to the current flow. The current difference between IR $= 50$ mW and IR $= 0$ was denoted as photocurrent ($Iphoto$) in the following discussion.

The relationship between gate voltage and photocurrent at zero bias for this symmetric CNTFET is shown in Fig. 4(b). One important feature observed is the photocurrent was negative and enhanced by increasing positive gate voltage, while became positive when negative gate voltage was applied. This can be understood by the schematic band diagram shown in Fig. 4(b). If positive gate voltage was applied, the Fermi energy of the nanotube was lower than the work function of Au, since positive gate voltage decreased the Fermi energy of the SWCNT. In contrast, sufficient negative gate voltage would make the Fermi energy of nanotube higher than the work function of Au. As a result, the direction of the Schottky barrier changed, causing the photocurrent direction change. The photocurrent polar change was also observed in silicon-nanowire transistor owing to the

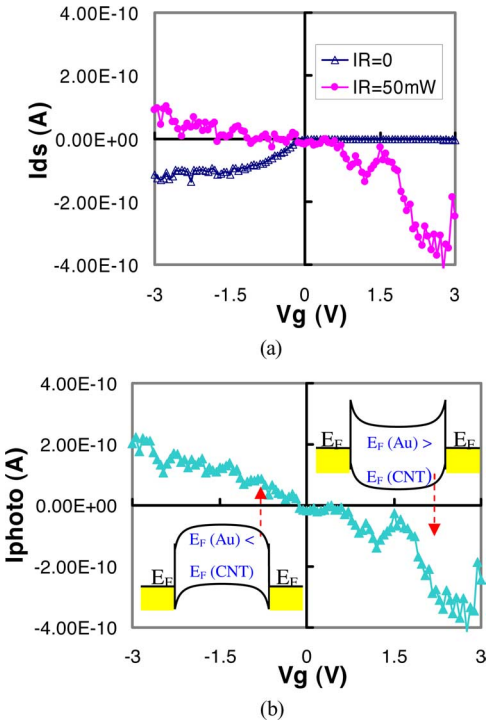

Fig. 4. (a) Transfer characteristic of the Au-CNT-Au CNTFET with IR source OFF (IR = 0) and ON (IR = 50 mW) at zero bias. (b) Relationship between gate voltage and photocurrent and corresponding band diagrams at negative and positive gate voltages.

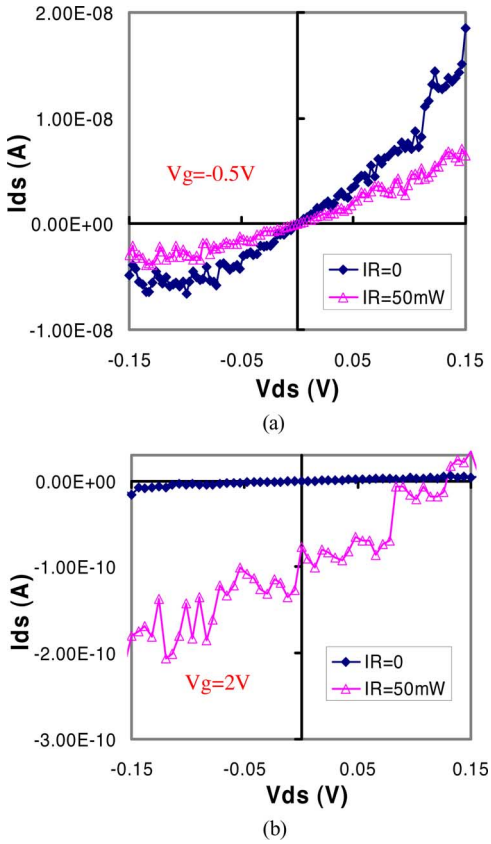

Fig. 5. Bias dependent measurement of the Au-CNT-Au CNTFET with IR = 0 and IR = 50 mW at (a) $V_g = -0.5$ V and (b) $V_g = 2$ V.

modification of energy alignment [45]. In addition, the result in Fig. 4(b) verified that the work functions of Au and SWCNT were very close, since the photocurrent at zero gate voltage was approximately −17.5 pA, and a very small negative gate voltage (∼-0.2 V) was able to change the direction of the photocurrent (2.35 pA, not shown in Fig. 4).

It was also observed that the magnitude of photocurrent was enhanced with increasing magnitude of both positive and negative gate voltages. However, the photocurrent to dark current ratio (denoted as ON/OFF ratio in the following discussion) at positive gate voltage are much higher than that at negative gate voltage, as explained in the following.

For negative gate voltage, increasing gate voltage will result in higher built-in potential and p-doping level. The additional p-doping may turn the SWCNT into a degenerated doped semiconductor because CNT is a p-type material in the air [46]. The bias-dependent photocurrent at $V_g = -0.5$ V was measured and shown in Fig. 5(a). One distinct feature was that the conductance decreased with excess carrier generation under IR illumination, which is caused by the contradiction of the separated photogenerated and injection carriers. In addition, higher bias resulted in higher photocurrent because the bias decreased the carrier-transit time that achieved photoconductive gain.

For positive gate voltage, larger voltage will result in higher built-in potential but lower p-doping level. It has shown that depletion width varied exponentially with inverse doping [30] and built-in potential [47]. Therefore, the photocurrent at positive gate voltage was increased by the widened depletion region, which enlarged the effective absorption area. As a result, the ON/OFF ratio at positive gate voltage was highly improved due to the suppression of dark current and enhancement of photocurrent. The bias dependent measurement at $V_g = 2$ V is shown in Fig. 5(b), which showed clearly photovoltaic characteristics: negative bias increased the photocurrent, while positive bias decreased the photocurrent. At $V_{ds} = 0.12$ V, the photocurrent was equal to the current produced by the bias, resulting in zero net current. This bias is the open-circuit voltage, denoted as V_{oc}.

A CNTFET using Ag electrodes was also fabricated to investigate the role of metal-work function. It has similar electrical characteristics (p-FET) to the Au-CNT-Au transistor. However, the conductance of the Ag-CNT-Ag CNTFET was ∼1–2 order magnitude smaller than the Au-based transistor. This can be understood by suppressed tunneling probability through higher and wider Schottky barriers between Ag and SWCNT [48], since Ag has lower work function (Ag = 4.2–4.5 eV) [49] that will result in a higher built-in potential.

The relation between gate voltage and photocurrent was measured and shown in Fig. 6(a). It was observed that the positive gate voltage not only suppressed dark current (in p-FET), but also increased the photocurrent. As a result, the ON/OFF ratio was highly improved. The open-circuit voltage at zero gate voltage was small, however, a 0.3 V open-circuit voltage was observed when a gate voltage of 3 V was applied to the silicon substrate and illuminated by an IR laser with 50 mW output

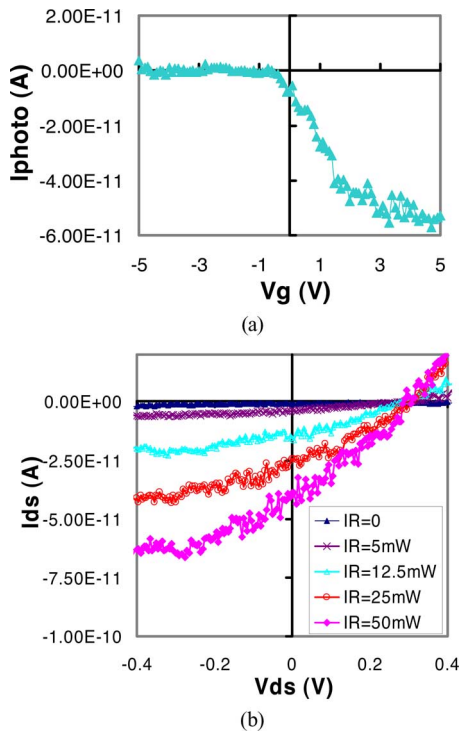

Fig. 6. (a) Relation between gate voltage and photocurrent of the Ag-CNT-Ag CNTFET at zero bias. (b) Bias dependent measurement with IR at five different output powers at $V_g = 3$ V.

power, as shown in Fig. 6(b) that conducted bias dependent measurement with five different power output.

It was noticed that the photocurrent of the Ag-CNT-Ag photodetector at IR = 50 mW and zero bias (5×10^{-11} A) was smaller than the Au-CNT-Au CNTFET (1×10^{-10} A) in the bias-dependent measurements, but the open-circuit voltage was higher. This is caused by the symmetric structure, a higher built-in potential in Ag-nanotube contacts resulted in wider absorption width (depletion width) and lower dark current, but the separated electron-hole at one barrier also needed to tunnel through a wider barrier in order to contribute to photocurrent flow, which is supported by the experimental results of illuminating photons at different positions of the detectors [23].

C. Asymmetric Ag-CNT-Au CNTFET Infrared Detector

The symmetric structure severely depressed the generation of photocurrent, since photogenerated electrons and holes need to tunnel a wide barrier before being collected. An asymmetric CNTFET can solve this problem by using Au electrode as source and Ag electrode as drain, resulting in two unbalanced barriers.

This can be understood by the band diagram of the asymmetric Ag-CNT-Au CNTFET as shown in Fig. 7. This detector will behave like a Schottky diode, and its optoelectronic properties will be dominated by the Schottky barrier between Ag and CNT [50]. When IR-laser spot was focused on the Ag-nanotube contact, photoresponse can be improved since the separated electrons and holes do not need to pass through a strong barrier (Ag-nanotube) as in the Ag-CNT-Ag structure.

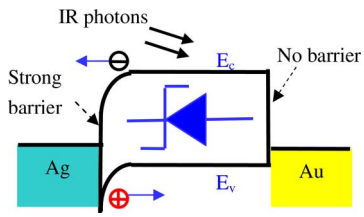

Fig. 7. Band diagram of the asymmetric CNTFET photodetector.

This design was based on the results of Section II-B, but the SWCNTs used for those measurements were different. Although they have similar diameter, their properties may vary due to the chirality difference or defects. In order to verify the concept of this asymmetric IR detector, a fabrication process was designed that allowed to measure the electrical properties of both Au-CNT-Au and Ag-CNT-Au FETs using an individual SWCNT.

The cross section of the device is shown in Fig. 8(a). At the beginning, two Au electrodes with a gap of 1.2 μm will be developed using ebeam lithography and deposited on top of a heavily doped Si/SiO_2 substrate. It was followed by depositing an individual SWCNT bridging these two electrodes using the DEP and AFM manipulation system. The *I–V* characteristics were measured denoted as Au-CNT-Au in Fig. 8(c). After that, another ebeam lithography was done to pattern and deposit an Ag electrode that covered one of the Au electrodes and extend 0.2 μm into the gap, making the device structured as Ag-CNT-Au with a gap of 1.0 μm, as shown in Fig. 8(b). Its electrical characteristics were measured and shown in Fig. 8(c) denoted as Ag-CNT-Au. The Au-CNT-Au showed symmetric and quasi-metallic electrical characteristics (weak parabolic *I–V* characteristics with higher bias), while typical diode electrical characteristics were observed in the Ag-CNT-Au structure. The electrical properties and conductance of the device were varied significantly due to the replacement of an Au electrode using an Ag electrode. Therefore, there must be a higher barrier between Ag and nanotube that dominates the optoelectronics properties of the detector [51].

This asymmetric detector fabrication can be simplified using a similar process as the symmetric CNTFET. The difference was fabricating only one Au electrode first, and was followed by making an Ag electrode with a gap of around 1 μm to the Au electrode after precise alignment using photolithography.

The transfer characteristics of an asymmetric CNTFET photodetector using an individual SWCNT at zero bias are shown in Fig. 9(a) with IR illumination power of 0 and 50 mW, respectively. The dark current showed p-FET characteristics. One particular characteristic was the improvement of the photocurrent. The photocurrent in Fig. 9(b) did not show obvious improvement due to the hysteresis effect [52]. The temporal photoresponse is shown in Fig. 9(b), which shows that the photocurrent was improved from 2×10^{-11} A ($V_g = 0$ V) to 1.2×10^{-9} A ($V_g = 8$ V). The highest photocurrent, obtained at positive gate voltage with a value of around 1 nA, was an order magnitude higher than the highest photocurrent of symmetric detectors. It is also observed that the ON/OFF ratio of this asymmetric detector at $V_g = 8$ V is more than 1000, which is two-order magnitude higher

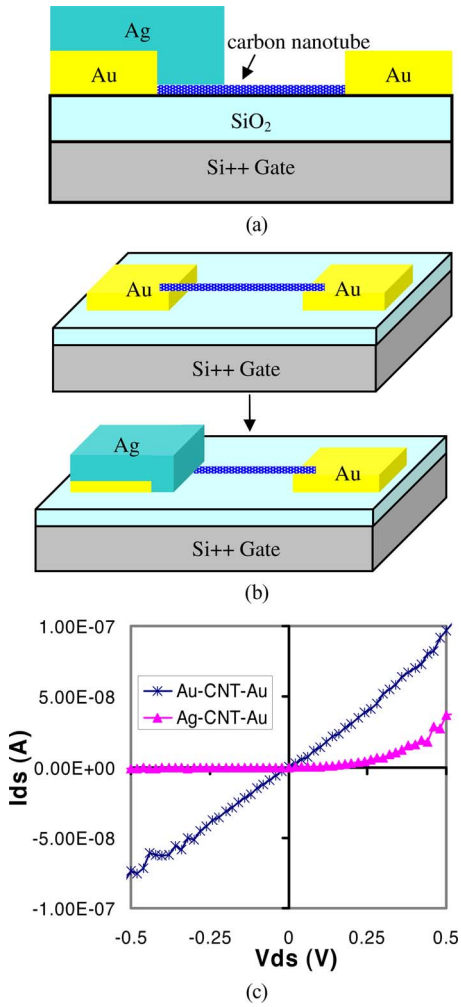

Fig. 8. (a) Cross section of the device that used to measure the electrical characteristics of Au-CNT-Au and Ag-CNT-Au detectors. (b) Fabrication process. (c) Electrical characteristics of Au-CNT-Au and Ag-CNT-Au detectors.

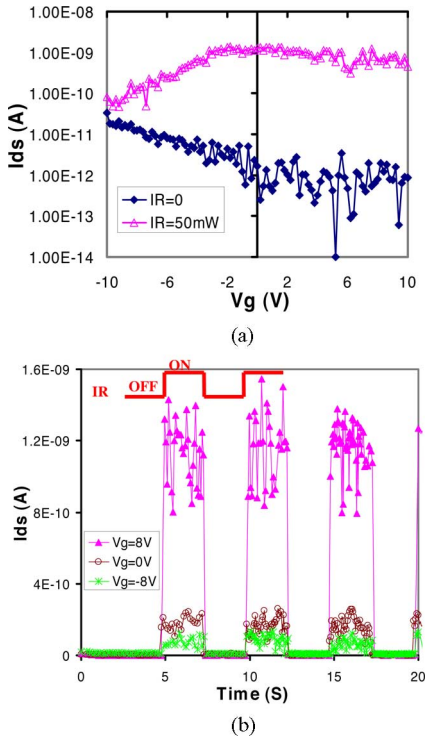

Fig. 9. (a) Transfer characteristic of the asymmetric CNTFET with and without IR illumination. (b) Temporal photoresponse with three different gate voltages at IR = 50 mW.

than the symmetric photodiode shown in Fig. 1. As a result, the open-circuit voltage was expected to be improved. The bias-dependent measurement with five different output powers at $V_g = 5$ V is shown in Fig. 10. This is a typical photovoltaic photoresponse electrical characteristics. The open-circuit voltage with 50 mW IR illumination was around 0.45 V, which is the highest open-circuit voltage reported for an individual nanotube-based photodetector to date. In contrast to the photocurrent that exceptionally depends on the absorbed number of photons, the open-circuit voltage is determined by the ON/OFF ratio, which can be high even absorbing small amount of photons because the dark current can be extremely low due to its nanoscale size and phonon-scattering suppression in 1-D structure.

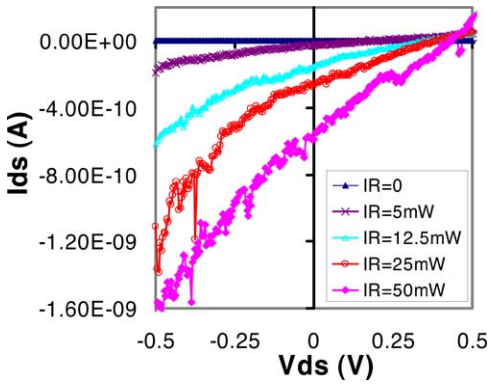

Fig. 10. Bias dependent measurement with IR at five different output powers at $V_g = 5$ V.

TABLE I
PERFORMANCE OF FOUR SWCNT DETECTORS

SWCNT Infared Detectors	Dark Current (A)	*Iphoto* (A)	*Voc* (V)
Au-CNT-Au Photodiode	1.5×10^{-12}	1.5×10^{-11}	~0
Au-CNT-Au CNTFET	5×10^{-13}	1×10^{-10}	0.12
Ag-CNT-Ag CNTFET	1×10^{-13}	5×10^{-11}	0.3
Ag-CNT-Au CNTFET	5×10^{-13}	1×10^{-9}	0.45

D. CNTFET IR Detector Performances and Analysis

The performance of two-symmetric and one-asymmetric IR detectors using CNTFET had been investigated in previous sections. The typical performance of four types of nanotube photodetectors at zero bias are summarized in Table I. The Au-CNT-Au photodiode introduced in this paper has dark current of 1.5×10^{-12} A and *Iphoto* of 1.5×10^{-11} A, with an ON/OFF ratio of ~10. It was found that the dark current and photocurrent were varying significantly in more than 20 Au-CNT-Au photodiodes due to the nanotube variation (work function, diameter, and chirality), but no open-circuit voltage has been observed in as-made photodiodes because of the small ON/OFF ratio. The Au-CNT-Au CNTFET was able to improve

TABLE II
DARK CURRENT OF THREE DIFFERENT DETECTORS

Infrared Detectors	Dark Current
QW Infrared Detector	$5\times10^{-3}A@300K$ [54]
	$1\times10^{-8}A@77K$[54]
QD Infrared Detector	$1\times10^{-8}A@293K$[57]
	$1\times10^{-13}A@78K$[57]
Ag-CNT-Au CNTFET Detector	$5\times10^{-13}A@300K$

photodiodes' performance by capacitively electrostatic doping. It was demonstrated that positive gate voltage can not only suppress dark current, but also increase photocurrent, and as a result an open-circuit voltage of 0.12 V was observed. Compared to the Au-CNT-Au CNTFET, the Ag-CNT-Ag CNTFET, albeit with larger Schottky barriers, did not generate higher photocurrent, since the separated electrons and holes from one Ag-nanotube barrier need to tunnel through another Ag-nanotube barrier before being collected in this symmetric structure. However, it highly decreased dark current due to a higher built-in potential and barrier height, and hence, increased the open-circuit voltage. A highest open-circuit voltage observed in the Ag-CNT-Ag CNTFET-based detector was 0.3 V with an applied-gate voltage. The problems associated with the symmetric photodetectors can be overcome by using asymmetric Ag-CNT-Au CNTFET. In this structure, the photogenerated electrons and holes from the Ag-nanotube contacts can mostly contribute to the photocurrent generation, because they only need to pass a small or no barrier between Au and nanotube. Consequently, photocurrent as well as open-circuit voltage were highly enhanced.

Both photocurrent and open-circuit voltage of CNT photosensors can be used to detect and quantify incident-IR signals. However, the photocurrent of nanotube photodetector is fairly small ($<$2 nA) compared to other bulk photodetectors due to the small absorption area of nanotube. However, the open-circuit voltage is of the same order as other bulk photodetectors [53] by taking advantage of the low dark current, since the open-circuit voltage depends on ON/OFF ratio [22]. Therefore, the 1-D photodetector has the potential to outperform traditional photodetectors, but with much smaller size, which is highly demanded in various fields.

A high open-circuit voltage can be obtained in these nanoscale photodetectors is owing to the extremely low dark current originated from the quantum confined 1-D structure of CNTs. Table II lists the dark currents of a quantum-well (QW) detector, quantum-dot (QD) detector, and asymmetric CNTFET detector. The QW photodetectors had attracted extensive attention and showed wide spectrum detection by utilizing intersubband absorption instead of interband absorption mechanism [54]. However, there are some problems associated with the QW structure, and one primary problem is their high dark currents [55] even in cryogenic temperature, as shown in Table II. QD photodetectors have the potential to produce lower dark current due to a lower activation energy [55] and 3-D phonon-scattering suppression [56]. Table II shows the QD photodetector has 5-order magnitude lower dark current than the QW photodetector. However, most QW and QD photodetectors need to operate in cryogenic temperature. CNT photodetectors has much smaller size than those detectors, and its 1-D structure will suppress phonon scattering within the nanotube, thus, they have much lower dark current at room temperature. In addition, the photogenerated carriers in 1-D photodetectors have longer life time and lower transit time [15], which can potentially improve the operating temperature. It was demonstrated that the CNT photodetectors were capable to sense both near-IR and midIR signals at room temperature [17]. CNTFET shows great promise to make miniature photosensors with high sensitivity.

III. CONCLUSION

In summary, three types of CNTFETs were fabricated to investigate and improve the performance of the nanoscale IR detectors using an individual SWCNT. In the Au-CNT-Au CNTFET, the sensor performance was improved by applying gate voltage to widen the 1-D Schottky barriers through modifying the doping level of nanotube electrostatically. The Ag-CNT-Ag CNTFET had higher open-circuit voltage when illuminated by IR laser, since the built-in potential in the Ag-nanotube interface is higher than that of the Au-nanotube, showing the importance of metal-work function. However, in the symmetric CNTFETs, separated electrons and holes need to tunnel through another Schottky barrier, severely constraining their sensitivity. In the asymmetric Ag-CNT-Au CNTFET-based detector, both photocurrent and open-circuit voltages were highly improved, since the electrons and holes from the Ag-nanotube interface only need to pass through a small barrier between Au and nanotube before being collected, showing a highest open-circuit voltage (0.45 V) reported to date. The theoretical analyses as well as experimental results have shown that the CNT can become important building blocks for nanoscale IR sensors.

REFERENCES

[1] S. Iijima, "Helical microtubules of graphitic carbon," *Nature*, vol. 354, pp. 56–58, 1991.
[2] N. Sinha and J.-W. Yeow, "Carbon nanotubes for biomedical applications," *IEEE Trans. NanoBiosci.*, vol. 4, no. 2, pp. 180–195, Jun. 2005.
[3] K. Besteman, J.-O. Lee, F. G. M. Wiertz, H. A. Heering, and C. Dekker, "Enzyme-coated carbon nanotubes as single-molecule biosensors," *Nano Lett.*, vol. 3, pp. 727–730, 2003.
[4] L. Valentini, I. Armentano, J. M. Kenny, C. Cantalini, L. Lozzi, and S. Santucci, "Sensors for sub-ppm no2 gas detection based on carbon nanotube thin films," *Appl. Phys. Lett.*, vol. 82, pp. 961–963, 2003.
[5] J. Li, Y. Lu, Q. Ye, M. Cinke, J. Han, and M. Meyyappan, "Carbon nanotube sensors for gas and organic vapor detection," *Nano Lett.*, vol. 3, pp. 929–933, 2003.
[6] J. R. Wood and H. D. Wagner, "Single-wall carbon nanotubes as molecular pressure sensors," *Appl. Phys. Lett.*, vol. 76, no. 20, pp. 2883–2885, 2000.
[7] C. Y. Li and T. W. Chou, "Strain and pressure sensing using single-walled carbon nanotubes," *Nanotechnology*, vol. 15, no. 11, pp. 1493–1496, 2004.
[8] S. J. Wind, J. Appenzeller, R. Martel, V. Derycke, and P. Avouris, "Vertical scaling of carbon nanotube field-effect transistors using top gate electrodes," *Appl. Phys. Lett.*, vol. 80, pp. 3817–3819, 2002.
[9] A. Javey, J. Guo, D. Farmer, Q. Wang, D. Wang, R. Gordon, M. Lundstrom, and H. Dai, "Carbon nanotube field-effect transistors with integrated ohmic contacts and high-k gate dielectrics," *Nano Lett.*, vol. 4, no. 3, pp. 447–450, 2004.
[10] J. A. Misewich, R. Martel, P. Avouris, J. C. Tsang, S. Heinze, and J. Tersoff, "Electrically induced optical emission from a carbon nanotube FET," *Science*, vol. 300, no. 5620, pp. 783–786, 2003.

[11] M. E. Itkis, F. Borondics, A. Yu, and R. C. Haddon, "Bolometric infrared photoresponse of suspended single-walled carbon nanotube films," *Science*, vol. 312, no. 5772, pp. 413–416, 2006.
[12] C. K. M. Fung, N. Xi, B. Shanker, and K. W. C. Lai, "Nanoresonant signal boosters for carbon nanotube based infrared detectors," *Nanotechnology*, vol. 20, no. 18, p. 185201, 2009.
[13] U. Bockelmann and G. Bastard, "Phonon scattering and energy relaxation in two-, one-, and zero-dimensional electron gases," *Phys. Rev. B*, vol. 42, no. 14, pp. 8947–8951, 1990.
[14] D. Kuo, A. Fang, and Y. Chang, "Theoretical modeling of dark current and photo-response for quantum well and quantum dot infrared detectors," *Infrared Phys. Technol.*, vol. 42, pp. 422–433, 2001.
[15] C. A. Soci, A. A. Zhang, B. A. Xiang, S. A. A. Dayeh, D. P. R. A. Aplin, J. A. Park, X. Y. A. Bao, Y. H. A. Lo, and D. Y. Wang, "Zno nanowire uv photodetectors with high internal gain," *Nano Lett.*, vol. 7, pp. 1003–1009, 2007.
[16] P. G. Collins, M. S. Arnold, and P. Avouris, "Engineering carbon nanotubes and nanotube circuits using electrical breakdown," *Science*, vol. 292, no. 5517, pp. 706–709, 2001.
[17] K. W. C. Lai, N. Xi, C. K. M. Fung, H. Chen, and T.-J. Tarn, "Engineering the band gap of carbon nanotube for infrared sensors," *Appl. Phys. Lett.*, vol. 95, no. 22, pp. 221107-1–221107-3, 2009.
[18] K. Lai, N. Xi, C. Fung, H. Chen, and T. Tarn, "Development of carbon nanotube based spectrum infrared sensors," in *Proc. IEEE Nanotechnol. Mater. Devices Conf.*, Jun. 2–5, 2009, pp. 130–135.
[19] F. M. C. Léonard and J. Tersoff, "Role of fermi-level pinning in nanotube schottky diodes," *Phys. Rev. Lett.*, vol. 84, no. 20, pp. 4693–4696, 2000.
[20] I. A. Levitsky and W. B. Euler, "Photoconductivity of single-wall carbon nanotubes under continuous-wave near-infrared illumination," *Appl. Phys. Lett.*, vol. 83, pp. 1857–1859, 2003.
[21] A. Fujiwara, Y. Matsuoka, H. Suematsu, N. Ogawa, K. Miyano, H. Kataura, Y. Maniwa, S. Suzuki, and Y. Achiba, "Photoconductivity in semiconducting single-walled carbon nanotubes," *Jpn. J. Appl. Phys.*, vol. 40, no. Part 2, no. 11B, pp. L1229–L1231, 2001.
[22] J. U. Lee, "Photovoltaic effect in ideal carbon nanotube diodes," *Appl. Phys. Lett.*, vol. 87, pp. 073101-1–073101-3, 2005.
[23] J. Zhang, N. Xi, H. Chen, K. W. C. Lai, G. Li, and U. Wejinya, "Photovoltaic effect in single carbon nanotube-based schottky diodes," *Int. J. Nanoparticles*, vol. 1, no. 2, pp. 108–118, 2008.
[24] H. Dai, "Carbon nanotubes: Synthesis, integration, and properties," *Acc. Chem. Res.*, vol. 35, pp. 1035–1044, 2002.
[25] M. Freitag, Y. Martin, J. A. Misewich, R. Martel, and P. Avouris, "Photoconductivity of single carbon nanotubes," *Nano Lett.*, vol. 3, pp. 1067–1071, 2003.
[26] X. Qiu, M. Freitag, V. Perebeinos, and P. Avouris, "Photoconductivity spectra of single-carbon nanotubes: Implications on the nature of their excited states," *Nano Lett.*, vol. 5, pp. 749–752, 2005.
[27] H. Chen, N. Xi, K. Lai, C. Fung, and R. Yang, "Cnt infrared detectors using schottky barriers and p-n junctions based fets," in *Proc. IEEE Nanotechnol. Mater. Devices Conf.*, Jun. 2–5, 2009, pp. 91–95.
[28] R. Martel, T. Schmidt, H. R. Shea, T. Hertel, and P. Avouris, "Single- and multi-wall carbon nanotube field-effect transistors," *Appl. Phys. Lett.*, vol. 73, no. 17, pp. 2447–2449, 1998.
[29] A. Javey, J. Guo, Q. Wang, M. Lundstrom, and H. Dai, "Ballistic carbon nanotube field-effect transistors," *Nature*, vol. 424, pp. 654–657, 2003.
[30] F. m. c. Léonard and J. Tersoff, "Novel length scales in nanotube devices," *Phys. Rev. Lett.*, vol. 83, no. 24, pp. 5174–5177, 1999.
[31] X. Cui, M. Freitag, R. Martel, L. Brus, and P. Avouris, "Controlling energy-level alignments at carbon nanotube/au contacts," *Nano Lett.*, vol. 3, pp. 783–787, 2003.
[32] J. Zhao, J. Han, and J. P. Lu, "Work functions of pristine and alkali-metal intercalated carbon nanotubes and bundles," *Phys. Rev. B*, vol. 65, no. 19, pp. 193401-1–193401-4, 2002.
[33] R. Gao, Z. Pan, and Z. L. Wang, "Work function at the tips of multiwalled carbon nanotubes," *Appl. Phys. Lett.*, vol. 78, no. 12, pp. 1757–1759, 2001.
[34] Y.-M. Lin, J. Appenzeller, J. Knoch, and P. Avouris, "High-performance carbon nanotube field-effect transistor with tunable polarities," *IEEE Trans. Nanotechnol.*, vol. 4, no. 5, pp. 481–489, Sep. 2005.
[35] K. W. C. Lai, N. Xi, and U. C. Wejinya, "Automated process for selection of carbon nanotube by electronic property using dielectrophoretic manipulation," *J. Micro-Nano Mechatron.*, vol. 4, no. 1–2, pp. 37–48, 2008.
[36] G. Y. Li, N. Xi, and M. Yu, "Development of augmented reality system for afm based nanomanipulation," *IEEE/ASME Trans. Mechatronics*, vol. 9, no. 2, pp. 358–365, Jun. 2004.
[37] J. Zhang, N. Xi, G. Li, H. Y. Chan, and U. C. Weijinya, "Adaptable end effector for atomic force microscopy based nanomanipulation," *IEEE Trans. Nanotechnol.*, vol. 5, no. 6, pp. 628–642, Nov. 2006.
[38] J. Zhang, N. Xi, L. Liu, H. Chen, K. Lai, and G. Li, "Atomic force yields a master nanomanipulator," *IEEE Nanotechnol. Mag.*, vol. 2, no. 2, pp. 13–17, Jun. 2008.
[39] J. Zhang, N. Xi, H. Chen, K. Lai, G. Li, and U. Wejinya, "Design, manufacturing, and testing of single-carbon-nanotube-based infrared sensors," *IEEE Trans. Nanotechnol.*, vol. 8, no. 2, pp. 245–251, Mar. 2009.
[40] K. W. C. Lai, N. Xi, C. K. M. Fung, J. Zhang, H. Chen, Y. Luo, and U. C. Wejinya, "Automated nanomanufacturing system to assemble carbon nanotube based devices," *Int. J. Robot. Res.*, vol. 28, no. 4, pp. 523–536, 2009.
[41] M. Shiraishi and M. Ata, "Work function of carbon nanotubes," *Carbon*, vol. 39, no. 12, pp. 1913–1917, 2001.
[42] X. Cui, M. Freitag, R. Martel, L. Brus, and P. Avouris, "Controlling energy-level alignments at carbon nanotube/Au contacts," *Nano Lett.*, vol. 3, no. 6, pp. 783–787, 2003.
[43] J. Appenzeller, M. Radosavljević, J. Knoch, and P. Avouris, "Tunneling versus thermionic emission in one-dimensional semiconductors," *Phys. Rev. Lett.*, vol. 92, no. 4, pp. 048301-1–048301-4, 2004.
[44] V. Derycke, R. Martel, J. Appenzeller, and P. Avouris, "Controlling doping and carrier injection in carbon nanotube transistors," *Appl. Phys. Lett.*, vol. 80, no. 15, pp. 2773–2775, 2002.
[45] Y. Ahn, J. Dunning, and J. Park, "Scanning photocurrent imaging and electronic band studies in silicon nanowire field effect transistors," *Nano Lett.*, vol. 5, no. 7, pp. 1367–1370, 2005.
[46] D. Kang, N. Park, J. hye Ko, E. Bae, and W. Park, "Oxygen-induced p-type doping of a long individual single-walled carbon nanotube," *Nanotechnology*, vol. 16, no. 8, pp. 1048–1052, 2005.
[47] C. Chen, W. Zhang, E. S.-W. Kong, and Y. Zhang, "Carbon nanotube photovoltaic device with asymmetrical contacts," *Appl. Phys. Lett.*, vol. 94, no. 26, pp. 263501-1–263501-3, 2009.
[48] Z. Chen, J. Appenzeller, J. Knoch, Y. Lin, and P. Avouris, "The role of metal-nanotube contact in the performance of carbon nanotube field-effect transistors," *Nano Lett.*, vol. 5, no. 7, pp. 1497–1502, 2005.
[49] M. Chelvayohan and C. H. B. Mee, "Work function measurements on (110), (100) and (111) surfaces of silver," *J. Phys. C: Solid State Phys.*, vol. 15, no. 10, pp. 2305–2312, 1982.
[50] C. Lu, L. An, Q. Fu, J. Liu, H. Zhang, and J. Murduck, "Schottky diodes from asymmetric metal-nanotube contacts," *Appl. Phys. Lett.*, vol. 88, pp. 133501-1–133501-3, 2006.
[51] M. H. Yang, K. B. K. Teo, and W. I. Milne, "Carbon nanotube schottky diode and directionally dependent field-effect transistor using asymmetrical contacts," *Appl. Phys. Lett.*, vol. 87, pp. 253116-1–253116-3, 2005.
[52] W. Kim, A. Javey, O. Vermesh, Q. Wang, Y. Li, and H. Dai, "Hysteresis caused by water molecules in carbon nanotube field-effect transistors," *Nano Lett.*, vol. 3, pp. 193–198, 2003.
[53] K. W. Johnston, A. G. Pattantyus-Abraham, J. P. Clifford, S. H. Myrskog, D. D. MacNeil, L. Levina, and E. H. Sargent, "Schottky-quantum dot photovoltaics for efficient infrared power conversion," *Appl. Phys. Lett.*, vol. 92, no. 15, pp. 151115-1–151115-3, 2008.
[54] B. F. Levine, "Quantum-well infrared photodetectors," *J. Appl. Phys.*, vol. 74, no. 8, pp. R1–R81, 1993.
[55] H. Liu, J.-Y. Duboz, R. Dudek, Z. Wasilewski, S. Fafard, and P. Finnie, "Quantum dot infrared photodetectors," *Phys. E: Low-Dimensional Syst. Nanostruct.*, vol. 17, pp. 631–633, 2003.
[56] S. Y. Wang, S. D. Lin, H. W. Wu, and C. P. Lee, "Low dark current quantum-dot infrared photodetectors with an algaas current blocking layer," *Appl. Phys. Lett.*, vol. 78, no. 8, pp. 1023–1025, 2001.
[57] E.-T. Kim, A. Madhukar, Z. Ye, and J. C. Campbell, "High detectivity inas quantum dot infrared photodetectors," *Appl. Phys. Lett.*, vol. 84, no. 17, pp. 3277–3279, 2004.

Authors' photographs and biographies not available at the time of publication.